Tom Simril
Vice President
Catawba Nuclear Station

Duke Energy
CN01VP / 4800 Concord Road
York, SC 29745

o: 803.701.3340
f: 803.701.3221
Tom.Simril@duke-energy.com

Serial: RA-22-0180 10 CFR 50.55a
July 7, 2022

U.S. Nuclear Regulatory Commission (NRC)
ATTN: Document Control Desk
Washington, DC 20555-0001

Catawba Nuclear Station, Unit No. 2
Renewed Facility Operating License No. NPF-52
Docket No. 50-414

SUBJECT: Supplement to Proposed Alternative to Use Reactor Vessel Head Penetration Embedded Flaw Repair for Life of Plant

References:

1. Relief Request RA-21-0145, "Proposed Alternative to Use Reactor Vessel Head Penetration Repair for Life of Plant," dated January 20, 2022 [Agencywide Document Access Management System (ADAMS) Accession No. ML22020A283]

Pursuant to 10 CFR 50.55a(z)(1), Duke Energy Carolinas, LLC (Duke Energy), in Reference 1 requested NRC approval for Catawba Nuclear Station (CNS), Unit 2, of a proposed alternative to ASME Code repair and replace requirements, on the basis that the proposed alternative provides an acceptable level of quality and safety. A fracture mechanics analysis was provided as Attachment 1 to Reference 1 and contained proprietary information to Westinghouse, Inc. that was requested to be withheld from public disclosure in accordance with 10 CFR 2.390. Attachment 2 to Reference 1 provided a publicly available version of the fracture mechanics analysis. Subsequently, some of the information that was categorized as proprietary in Reference 1 has been identified to be previously available to the public via other documentation. This letter provides a revised version of the Reference 1 attachments in which information that was not made available to the public has now been released. The revisions to the analysis are limited to the release of proprietary information, specifically regarding changing references to reflect publicly available information and removing brackets surrounding publicly available information in the non-proprietary version of the analysis. No technical content or discussion surrounding technical content for the analysis was revised and thus remains as-is from the Reference 1 submittal.

Attachment 1 contains a revised fracture mechanics analysis. Attachment 1 contains information proprietary to Westinghouse and is requested to be withheld from public acces under 10 CFR

2.390. A non-proprietary version of the fracture mechanics analysis is provided as Attachment 2. An affidavit attesting to the proprietary nature of Attachment 1 is included as Attachment 3.

Should you have any questions concerning this letter and its enclosure, please contact Mr. Ryan Treadway – Director, Fleet Licensing, at (980) 373-5783.

Sincerely,

Tom Simril
Site Vice President
Catawba Nuclear Station

Attachment:

1. WCAP-18708-P, "Technical Basis for Westinghouse Embedded Flaw Repair of Catawba Unit 2 Reactor Vessel Head Penetration Nozzles and Attachment Welds," Revision 1 (Proprietary)
2. WCAP-18708-NP, "Technical Basis for Westinghouse Embedded Flaw Repair of Catawba Unit 2 Reactor Vessel Head Penetration Nozzles and Attachment Welds," Revision 1 (Non-Proprietary)
3. Affidavit Attesting to Proprietary Nature of Information in Attachment 1

cc:

L. Dudes, USNRC, Region II Regional Administrator
Z. Stone, USNRC NRR Project Manager for CNS
J. Austin, USNRC Senior Resident Inspector for CNS

Attachment 2

WCAP-18708-NP, "Technical Basis for Westinghouse Embedded Flaw Repair of Catawba Unit 2 Reactor Vessel Head Penetration Nozzles and Attachment Welds," Revision 1 (Non-Proprietary)

WCAP-18708-NP
Revision 1

June 2022

Technical Basis for Westinghouse Embedded Flaw Repair of Catawba Unit 2 Reactor Vessel Head Penetration Nozzles and Attachment Welds

WCAP-18708-NP
Revision 1

Technical Basis for Westinghouse Embedded Flaw Repair of Catawba Unit 2 Reactor Vessel Head Penetration Nozzles and Attachment Welds

June 2022

Maria Rizzilli*
RV/CV Design and Analysis

Verifier: Geoffrey M. Loy*
RV/CV Design and Analysis

Reviewers: Anees Udyawar*
RV/CV Design and Analysis

Approved: Lynn A. Patterson, Manager*
RV/CV Design and Analysis

Electronically approved records are authenticated in the electronic document management system.

Westinghouse Electric Company LLC
1000 Westinghouse Drive
Cranberry Township, PA 16066, USA

FOREWORD

This document contains Westinghouse Electric Company LLC proprietary information and data which has been identified by brackets. Coding (a,c,e) associated with the brackets sets forth information which is considered proprietary.

The proprietary information and data contained within the brackets in this report were obtained at considerable Westinghouse expense and its release could seriously affect our competitive position. This information is to be withheld from public disclosure in accordance with the Rules of Practice 10 CFR 2.390 and the information presented herein is safeguarded in accordance with 10 CFR 2.390. Withholding of this information does not adversely affect the public interest.

This information has been provided for your internal use only and should not be released to persons or organizations outside the Directorate of Regulation and the Advisory Committee on Reactor Safeguards (ACRS) without the express written approval of Westinghouse Electric Company LLC. Should it become necessary to release this information to such persons as part of the review procedure, please contact Westinghouse Electric Company LLC, which will make the necessary arrangements required to protect the Company's proprietary interests.

Several locations in this topical report contain proprietary information. Proprietary information is identified and bracketed. For each of the bracketed locations, the reason for the proprietary classification is provided, using a standardized system. The proprietary brackets are labeled with three (3) different letters, "a", "c", and "e" per Westinghouse policy procedure BMS-LGL-84, which stand for:

a. The information reveals the distinguishing aspects of a process or component, structure, tool, method, etc. The prevention of its use by Westinghouse's competitors, without license from Westinghouse, gives Westinghouse a competitive economic advantage.

c. The information, if used by a competitor, would reduce the competitor's expenditure of resources or improve the competitor's advantage in the design, manufacture, shipment, installation, assurance of quality, or licensing of a similar product.

e. The information reveals aspects of past, present, or future Westinghouse- or customer-funded development plans and programs of potential commercial value to Westinghouse.

The non-proprietary information in the brackets is provided in the proprietary version of this report (WCAP-18708-P Revision 1).

RECORD OF REVISIONS

Revision	Date	Revision Description
0	December 2021	Original Issue
1	June 2022	Revision 1 of this WCAP includes editorial changes by reclassifying proprietary information for certain paragraphs per request by Duke during the NRC review of this document, see revision bars in the left margin. There are no technical changes in the report that impact the inputs, methodology, results, or conclusions.

TABLE OF CONTENTS

1 INTRODUCTION

Leakage and cracks have been reported from the reactor vessel closure head penetration nozzles in a number of plants that resulted in repairs or prompted the replacement of the reactor vessel closure head. The degradation of the reactor vessel closure head penetration nozzles increases the probability of a more significant loss of reactor coolant pressure boundary. This has led to the issuance of various regulatory requirements and guidelines in the United States imposing additional volumetric and surface examinations to supplement the existing visual inspections of the reactor vessel closure head as well as the penetration nozzles. The presence of axial cracks extending above and below the head penetration nozzle attachment J-groove welds was discovered in some of the leaking penetration nozzles. The cause of these axially oriented cracks has been determined to result from primary water stress corrosion cracking (PWSCC) that is driven by both the steady state operating stress and the residual stress resulting from the weld fabrication process. The residual stress from the weld fabrication process is due to weld shrinkage and the offset geometry of the attachment J-groove weld on the uphill and downhill sides that induces bending of the penetration nozzle. The bending also contributes to the ovalization of the penetration nozzle over the attachment J-groove weld region.

As a part of the inspection and repair efforts associated with the reactor vessel closure head inspection program at Catawba Unit 2, engineering evaluations have been performed in this report to support plant-specific use of the Westinghouse embedded flaw repair process in the repair of unacceptable flaws. The embedded flaw repair process involves depositing a weld material that is PWSCC resistant over a detected flaw and the wetted surface of the penetration nozzle attachment J-groove weld. As a result, the surface flaw becomes a sub-surface flaw and is no longer exposed to the primary water environment. During Spring 2021 inspection of Catawba Unit 2 reactor vessel head, a surface indication on penetration 74 J-groove weld was identified which required an embedded flaw repair. The embedded flaw repair process, as completed for numerous other plants with similar indications, was completed for Catawba Unit 2. During this process, at least three weld layers of Alloy 52/52M repair weld material are deposited on the surface of the J-groove weld, thus making the indication an embedded flaw [1] and prompting the technical bases of the embedded flaw repair analysis. The analysis performed in this report provides technical justification for long term plant operation for Catawba Unit 2 reactor vessel head penetration 74 and all other penetrations where an embedded flaw repair is applied.

Section XI of the ASME Code did not have a provision for welding over an existing flaw until the 1992 Edition. Those plants inspecting to an earlier edition of the Code would have to process relief requests to use the embedded flaw repair method, or update to the 1992 Edition of the Code. The repair and replacements rules of IWA 4000 in Section XI, starting with the 1992 Edition, allow weld repair over an existing flaw, provided that the flaw can be shown to be acceptable to the analytical requirements of Section XI. Engineering evaluations were performed to determine the maximum flaw sizes that would satisfy the requirements in Section XI of the ASME Code [2] and be suitable to support the weld repair process. The results presented in this report would enable the weld repair team to effectively determine the appropriate repair method.

Section XI repair rules allow the use of grinding to remove flaws, regardless of the edition of the Code. The only requirement is to ensure that the excavated region still meets the stress limits of the original construction code, which was Section III. Evaluations were performed in [3] to provide repair guidelines that may be used for removal of defects found on the surfaces of J-groove attachment welds and associated nozzles for the Catawba Unit 2 control rod drive mechanism (CRDM) penetrations.

The technical basis of the embedded flaw repair process is documented in WCAP-15987-P [4], which has been reviewed and accepted by the NRC. The staff also concluded that WCAP-15987-P is acceptable for referencing in licensing applications. As discussed in Appendix C of WCAP-15987-P, Westinghouse has developed the following three repair scenarios/method to address the most common types of flaws during the vessel head inspection:

Scenario 1: Axial or circumferential crack in the penetration nozzle inner surface

Scenario 2: Postulated crack encompassing the entire penetration J-groove weld

Scenario 3: Axial or circumferential crack in the penetration nozzle outer surface

Figure 1-1 shows the repair for Scenario 1, and Figure 1-2 shows the repair for Scenario 2 and 3.

The purpose of this report is to provide plant-specific technical basis for the use of the embedded flaw repair process and to confirm that Catawba Unit 2 meets the criteria for application of the embedded flaw repair process stated in Appendix C of WCAP-15987-P [4]. Engineering evaluations were performed and the results are presented in this report to provide the maximum allowable initial embedded flaw sizes that could be repaired using the Westinghouse embedded flaw repair process and would satisfy the requirements in Section XI of the ASME Code [2]. The ASME Section XI Code of record for Catawba Unit 2 is 2007 Edition with 2008 Addenda [2]. Note that the methodology used in this report from the 2007 Edition with 2008 Addenda is the same up to the 2017 Edition of ASME Section XI Code, which is the most recent ASME Code edition approved by the NRC. The results presented in this report would support the use of the Westinghouse embedded flaw repair process as the repair option for all the Catawba Unit 2 reactor vessel head penetration nozzles. In this report, the technical basis and evaluation results to support the use of embedded flaw repair process for a flawed head penetration are provided in Section 2. The technical basis and evaluation results that support a similar application for a flawed head penetration nozzle attachment J-goove weld are provided in Section 3. The conclusions of this report are in Section 4, with supporting references in Section 5.

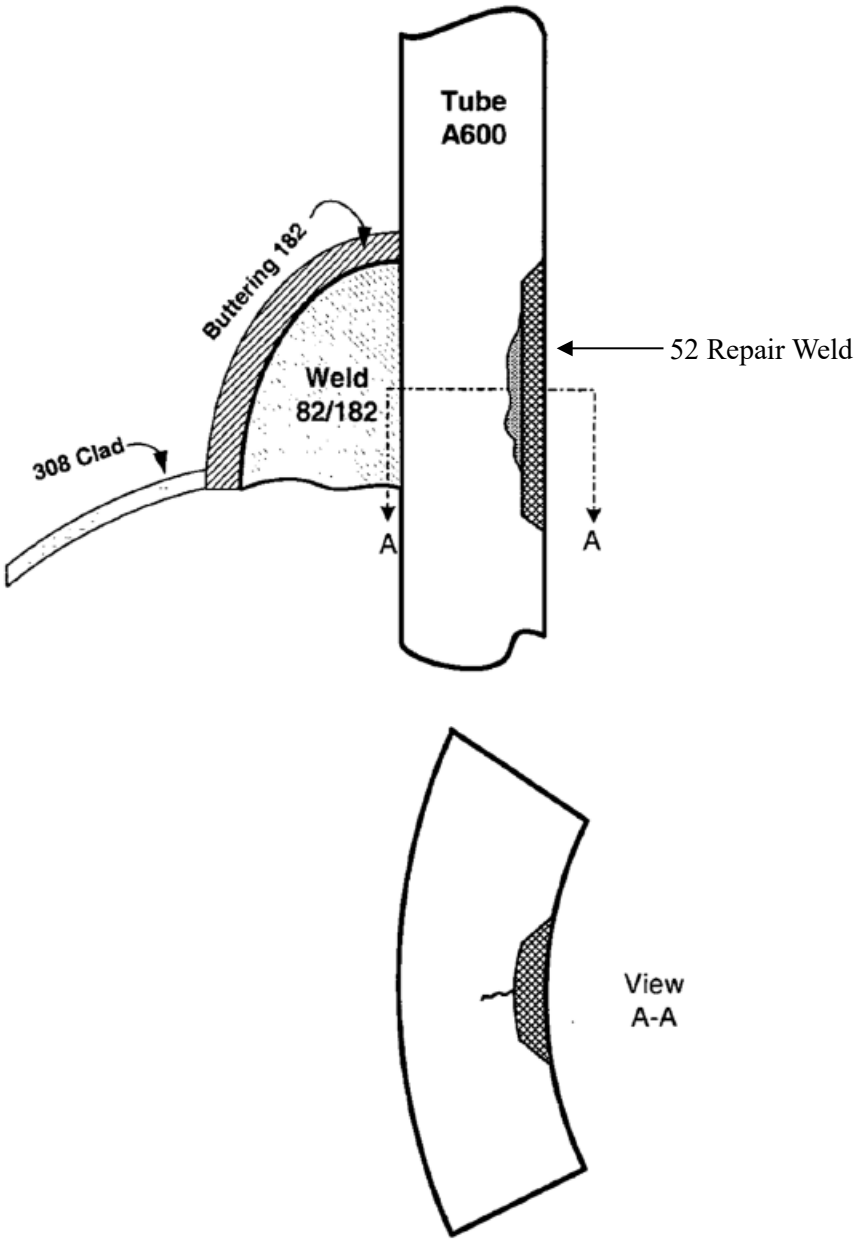

Figure 1-1 General Schematic of the Embedded Flaw Repair to a Flaw in the Head Penetration Tube Inside Surface

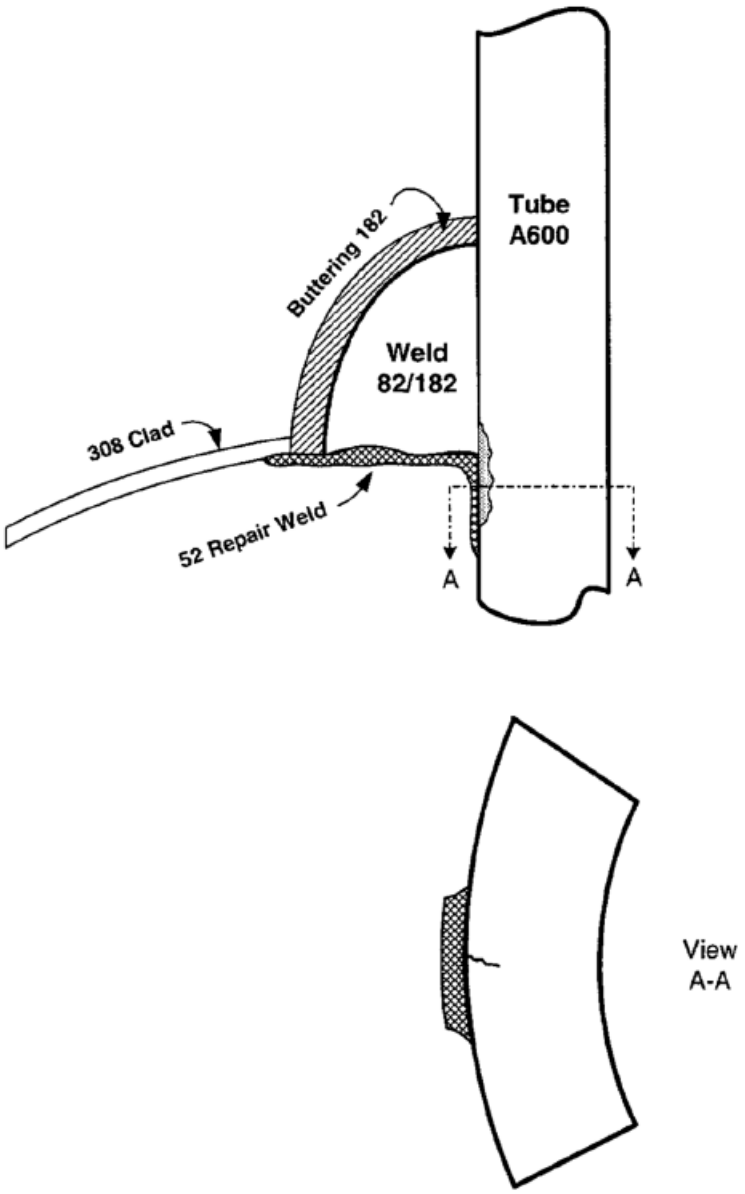

Figure 1-2 General Schematic of the Embedded Flaw Repair to a Flaw in the Head Penetration Tube Outside Surface, or to a Flaw in the Attachment Weld (J-Groove Weld)

2 TECHNICAL BASIS FOR APPLICATION OF EMBEDDED FLAW REPAIR TECHNIQUE TO PENETRATION NOZZLES

This section provides a discussion on the technical basis for the use of the embedded flaw repair method for a flawed head penetration nozzle (i.e., flaws on the inner diameter (ID) or outer diameter (OD) of the head penetration nozzles (Scenario 1 and Scenario 3)). Such a repair would involve depositing several layers of Alloy 52/52M weld material over the flaw detected on the inside surface of the penetration nozzle or right over the outside surface of the penetration nozzle of interest below the J-groove weld, as well as over the wetted surface of the J-groove weld in the event that an outside surface flaw is detected in the penetration nozzle. Since the Alloy 52/52M repair weld material is more PWSCC resistant than the existing Alloy 600 material, any detected surface flaws in the head penetration nozzles can then be shielded from the primary water environment and are no longer susceptible to primary water stress corrosion cracking. This is consistent with the current plant operation experiences that no primary water stress corrosion cracking initiation has been observed in Alloy 52/52M weld material so far. The technical basis for the use of the embedded flaw repair method for the flawed head attachment weld (Scenario 2) is provided in Section 3.

[

]^{a,c,e} This repair process is used to seal any potential flaws in the J-groove weld from further exposure to the primary water environment.

The evaluation of the embedded flaw repair for the axial or circumferential crack on the penetration inner surface (Scenario 1) or outer surface (Scenario 3) began with the determination of an allowable end-of-evaluation period flaw size based on the acceptance criteria described in Section 2.1 for a flaw postulated to remain in the repaired penetration nozzle. With the embedded flaw repair process, the only mechanism for sub-critical crack growth is fatigue. The maximum initial embedded flaw size that can remain in a repaired penetration nozzle using the embedded flaw repair process can then be determined by subtracting any predicted fatigue crack growth (FCG) for future plant operation (i.e., 20, 40, or 60 years) from the maximum allowable end-of-evaluation period flaw size. [

]^{a,c,e}

2.1 ACCEPTANCE CRITERIA

Rapid, non-ductile failure is possible for ferritic materials at low temperatures but is not applicable to the nickel-base alloy head penetration nozzle material, Alloy 600. Nickel-base alloy material is a high toughness material and plastic collapse would be the dominant mode of failure. [

]^{a,c,e}

2.1.1 Axial Flaws

For axial flaws the allowable flaw depth is given by [

]a,c,e

2.1.2 Circumferential Flaws

For circumferential flaws [

]a,c,e

2.2 METHODOLOGY

The evaluation assumed that an unacceptable flaw has been detected on the surface of a penetration nozzle and that the embedded flaw repair process is used to seal the flaw from further exposure to the primary water environment. The evaluation began with the determination of an allowable end-of-evaluation period flaw size based on the acceptance criteria described in Section 2.1 for a flaw postulated to remain in the repaired penetration nozzle. With the embedded flaw repair process, the only mechanism for sub-critical crack growth is fatigue. The maximum initial flaw size in a penetration nozzle that can be repaired using the embedded flaw repair process can then be determined by subtracting any predicted fatigue crack growth for future plant operation from the maximum allowable end-of-evaluation period flaw size. The following provides a discussion of the geometry, loading conditions, thermal transient stress analysis, and fatigue crack growth analysis used in the development of the plant specific technical basis for the embedded flaw repair process.

2.2.1 Geometry and Material

There are seventy eight CRDM head penetration nozzles in the reactor vessel upper closure head with the same nozzle geometry but at different locations in the closure head [5.a]. The outside radius and thickness for all Alloy 600 tubes are [ ]^{a,c,e} The CRDM nozzle material is SB-167 (per [5.d] and FSAR, Table 5-6 [9]).

2.2.2 Finite Element Analysis

The distributions of transient thermal and pressure stresses in the outermost reactor vessel head penetration nozzle were obtained from detailed three-dimensional elastic-plastic finite element analyses [6]. Reference [6] considers the welding residual stresses associated with original nozzle installation. Subsequent to the welding residual stress analysis, the stresses that result from the [ ]^{a,c,e} in the presence of welding residual conditions are calculated. [

]^{a,c,e} including the welding residual stresses associated with original nozzle installation. [

]^{a,c,e} Figure 2-2 shows the location of the stress cuts. [
]^{a,c,e} are used for the fatigue crack growth analysis of the circumferential and axial cracks postulated on the inside or outside of the nozzles.

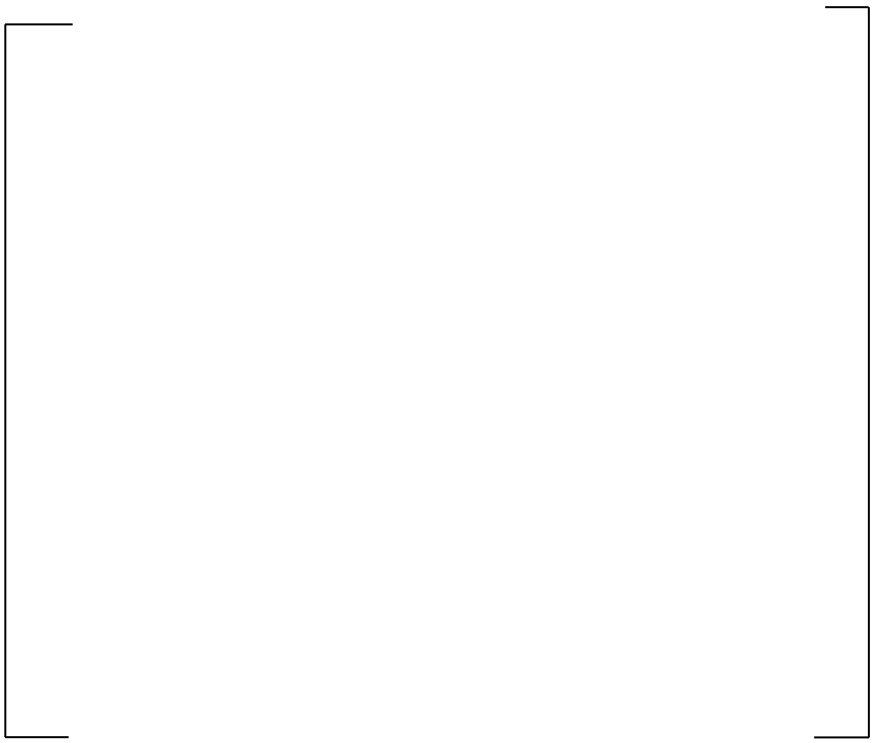

Figure 2-2 Finite Element Model with Analytical Stress Cuts Identified

2.2.3 Loading Conditions

The requirement for determining the maximum allowable end-of-evaluation period flaw size using the rules of Section XI is that the governing loadings from the normal, upset (including test), emergency, and faulted conditions be considered. This is necessary because, as discussed in Section 2.1, different safety margins are used for the normal/upset conditions and the emergency/faulted conditions. A lower safety factor is used to reflect the lower probability of occurrence for the emergency/faulted conditions.

[

]a,c,e

[

]^{a,c,e} The thermal transients that occur in the upper head region are relatively mild; Catawba Unit 2 is considered as a T_{cold} plant and the flow in the upper head region is low compared to other regions of the reactor vessel, which mutes the effects of the operating thermal transients. The normal, upset (including test), emergency, and faulted transients considered for Catawba Unit 2 reactor vessel analyses, design specifications [8.a and 8.b], and the design cycles of the transients from Table 3-50 of Catawba final safety analysis report (FSAR, Table 3-50) [9] are summarized in Table 2-1. [

]^{a,c,e}

Table 2-1 Catawba Unit 2 Design Transients

Transient	Cycles[1]
Plant Loading at 5% of Full Power/min	13,200[3]
Step Load Decrease of 10% Full Power	2,000
Step Load Increase of 10% Full Power	2,000
Large Step Load Decrease	200
Plant Unloading at 5% of Full Power/min	13,200[3]
Reactor Trip from Full Power	400
Reactor Trip with Cooldown (CD) and Safety Injection (SI)	10
Inadvertent Auxiliary Spray	10
Inadvertent Depressurization	20
Turbine Roll Test	10
Primary Side Leak Test	50
Loss of Flow	80
Loss of Power	40
Loss of Load from Full Power	80
Large Steam Line Break	1
Small Steam line Break	5
Small LOCA	5
Steady State Fluctuations	1,000,000[2]
Plant Heatup	200
Plant Cooldown	200

Notes:

1. Cycles are from Equipment Specifications [8.a and 8.b] unless otherwise noted.
2. The 1,000,000 cycles considered for the infinite steady state fluctuation transient.
3. Transient cycles based on Table 3-50 of Catawba final safety analysis report (FSAR) [9]

2.2.4 Allowable Flaw Size Determination

Allowable end-of-evaluation flaw sizes for axial and circumferential flaws with various aspect ratios (flaw length/flaw depth) in a CRDM penetration nozzle are calculated in accordance with the acceptance criteria discussed in Section 2.1. The allowable initial flaw sizes are subsequently determined by adjusting the allowable end-of-evaluation flaw sizes based on the results from the fatigue crack growth evaluation described in Section 2.2.6. Since the repaired flaws are embedded and sealed, they are not subjected to PWSCC.

2.2.5 Stress Intensity Factors

One of the key elements in a crack growth analysis is the crack driving force or crack tip stress intensity factor, K_I. This is based on the equations available in public literature. Both embedded and surface flaws are analyzed for repaired inside and outside surface flaws.

Outside and Inside Surface Flaws

The stress intensity factors (SIF), K_I, for the part through-wall surface cracks are calculated based on [ ]^{a,c,e} The stress distribution profile is represented by a 3rd order polynomial as shown below.

$$\sigma = \sigma_0 + \sigma_1 \left(\frac{a}{t}\right) + \sigma_2 \left(\frac{a}{t}\right)^2 + \sigma_3 \left(\frac{a}{t}\right)^3$$

where:

σ_0, σ_1, σ_2, and σ_3 are the stress profile curve fitting coefficients to be determined;

a is the distance from the wall surface where the crack initiates;

t is the wall thickness; and

σ is the stress perpendicular to the plane of the crack.

The SIFs can be expressed in the general form as follows:

[

]^{a,c,e}

Embedded Flaws

The stress intensity factor calculation for an embedded flaw was based on [

]^{a,c,e}

This stress intensity factor expression for subsurface (embedded) flaws can be expressed [

]a,c,e

2.2.6 Fatigue Crack Growth Prediction

With the application of the embedded flaw repair process, any postulated flaws in the reactor vessel head penetration tubes are sealed from the PWR environment; therefore, the only mechanism for crack growth would be due to fatigue crack growth.

The FCG analysis procedure involves postulating an initial flaw at the region of concern and predicting the growth of that flaw due to an imposed series of loading transients. The applied loads include pressure, thermal transients, and residual stresses. The normal, upset (including test), emergency, and faulted thermal transients as well as the associated design cycles considered in the fatigue crack growth analysis are shown in Table 2-1. The cycles are distributed evenly over 60 years of plant design life. The stress intensity factor range, ΔK_I, that controls fatigue crack growth, depends on the geometry of the crack, its surrounding structure, and the range of applied stresses in the region of the postulated crack. Once ΔK_I is calculated, the fatigue crack growth due to a particular stress cycle can be determined using a crack growth rate reference curve applicable to the material of the head penetration nozzle. Once the incremental crack growth corresponding to a specific transient is calculated for a small time period, it is added to the original crack size, and the analysis continues to the next time period and/or thermal transient. The procedure is repeated in this manner until all the significant analytical thermal transients and cycles known to occur in a given period of operation have been analyzed.

[

]a,c,e

2.3 FRACTURE MECHANICS ANALYSIS RESULTS

2.3.1 Maximum End-of-Evaluation Period Flaw Sizes

The maximum allowable end-of-evaluation period flaw sizes are determined for axial and circumferential surface flaws for postulated flaw aspect ratios (flaw length/flaw depth) of 2, 3, 6, and 10. The allowable flaw sizes are considered for all normal, upset, test, emergency, and faulted conditions and the most limiting allowable flaw sizes from these conditions are summarized in Table 2-2 and will be used in the generation of flaw evaluation charts.

Table 2-2 Maximum Allowable End-of-Evaluation Period Flaw Size Based on Section XI

Location	Aspect Ratio (l/a)	Axial Allowable Flaw Size		Circumferential Allowable Flaw Size	
		a/t	a (in.)	a/t	a (in.)
CRDM Nozzle [ ]a,c,e	2	0.75	0.469	0.75	0.469
	3	0.75	0.469	0.75	0.469
	6	0.75	0.469	0.58	0.363
	10	0.75	0.469	0.46	0.288

Notes: l = flaw length
a = flaw depth
t = wall thickness

2.3.2 Allowable Initial Flaw Sizes for Penetration Nozzles

After the maximum allowable end-of-evaluation period flaw sizes are determined, fatigue crack growth analyses are performed per the methodology discussed in Section 2.2. First, the outside and inside surface flaws with aspect ratios of 2, 3, 6, and 10 are postulated. [

]^{a,c,e} The results are also plotted in Figure 2-3 and Figure 2-4.

Table 2-3 Maximum Allowable Initial Flaw Size on CRDM Nozzle for Repair

Location	Years of Operation	Aspect Ratio (l/a)	Inside Surface				Outside Surface			
			Circumferential Flaw		Axial Flaw		Circumferential Flaw		Axial Flaw	
			a/t	a (in.)	a/t	a (in.)	a/t	a (in.)	a/t	a (in.)
Downhill Side	20	2	0.74	0.4625	0.74	0.4625	0.74	0.4625	0.74	0.4625
		3	0.74	0.4625	0.72	0.4500	0.73	0.4563	0.68	0.4250
		6	0.57	0.3563	0.64	0.4000	0.54	0.3375	0.52	0.3250
		10	0.45	0.2813	0.52	0.3250	0.42	0.2625	0.41	0.2563
	40	2	0.74	0.4625	0.74	0.4625	0.74	0.4625	0.73	0.4563
		3	0.74	0.4625	0.69	0.4313	0.72	0.4500	0.66	0.4125
		6	0.57	0.3563	0.57	0.3563	0.51	0.3188	0.47	0.2938
		10	0.45	0.2813	0.47	0.2938	0.39	0.2438	0.40	0.2500
	60	2	0.74	0.4625	0.73	0.4563	0.74	0.4625	0.72	0.4500
		3	0.74	0.4625	0.68	0.4250	0.71	0.4438	0.63	0.3938
		6	0.57	0.3563	0.54	0.3375	0.47	0.2938	0.44	0.2750
		10	0.45	0.2813	0.44	0.2750	0.37	0.2313	0.37	0.2313
Uphill Side	20	2	0.74	0.4625	0.73	0.4563	0.74	0.4625	0.72	0.4500
		3	0.74	0.4625	0.68	0.4250	0.73	0.4563	0.66	0.4125
		6	0.57	0.3563	0.53	0.3313	0.53	0.3313	0.46	0.2875
		10	0.45	0.2813	0.43	0.2688	0.43	0.2688	0.39	0.2438
	40	2	0.74	0.4625	0.71	0.4438	0.74	0.4625	0.70	0.4375
		3	0.74	0.4625	0.63	0.3938	0.72	0.4500	0.61	0.3813
		6	0.57	0.3563	0.46	0.2875	0.52	0.3250	0.42	0.2625
		10	0.45	0.2813	0.36	0.2250	0.40	0.2500	0.35	0.2188
	60	2	0.74	0.4625	0.7	0.4375	0.74	0.4625	0.68	0.4250
		3	0.74	0.4625	0.59	0.3688	0.71	0.4438	0.57	0.3563
		6	0.57	0.3563	0.41	0.2563	0.50	0.3125	0.38	0.2375
		10	0.45	0.2813	0.32	0.2000	0.38	0.2375	0.32	0.2000

Notes: l = flaw length
a = flaw depth
t = wall thickness

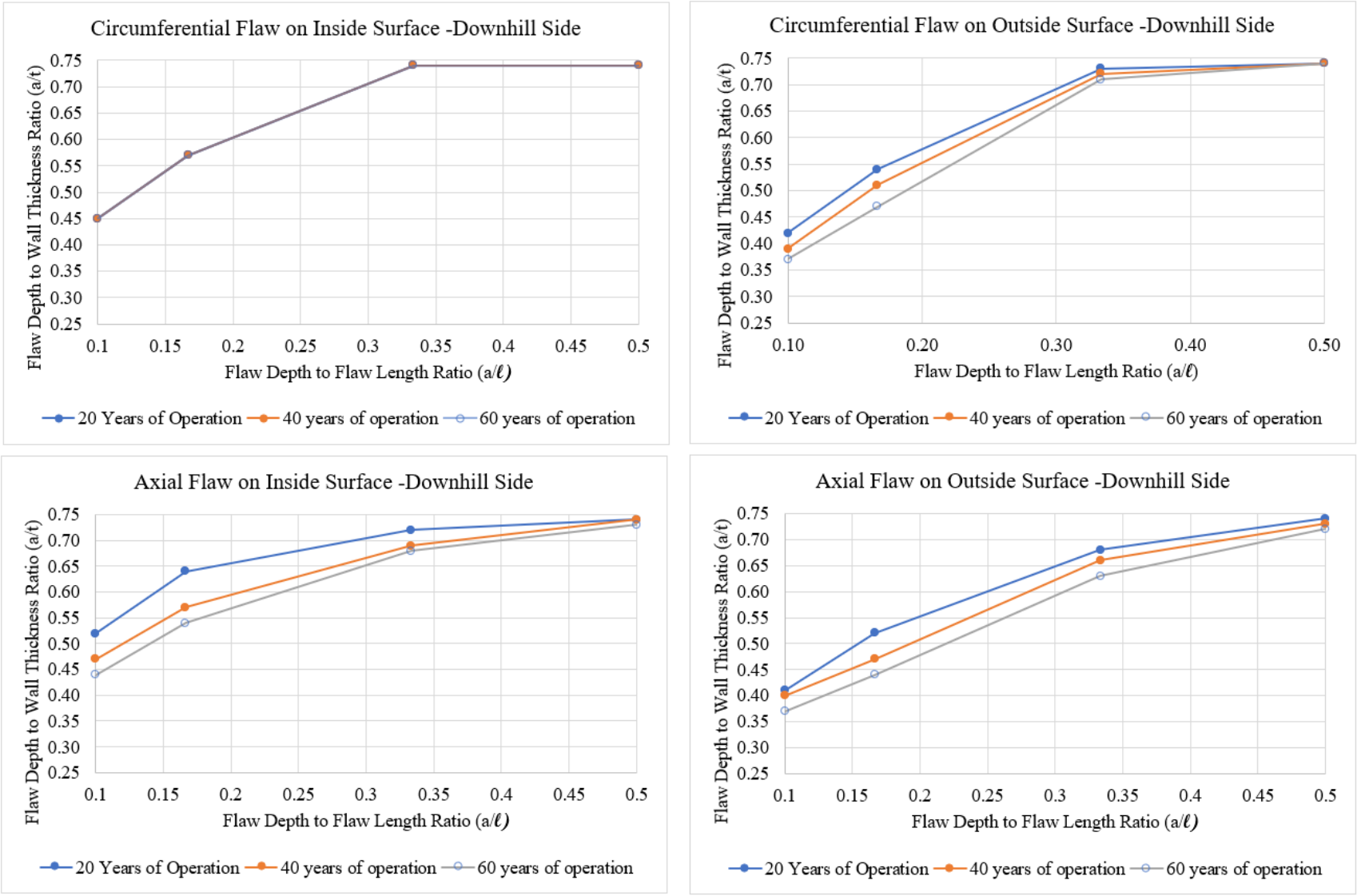

Figure 2-3 Maximum Allowable Initial Flaw Size on CRDM Nozzle for Repair – Downhill Side

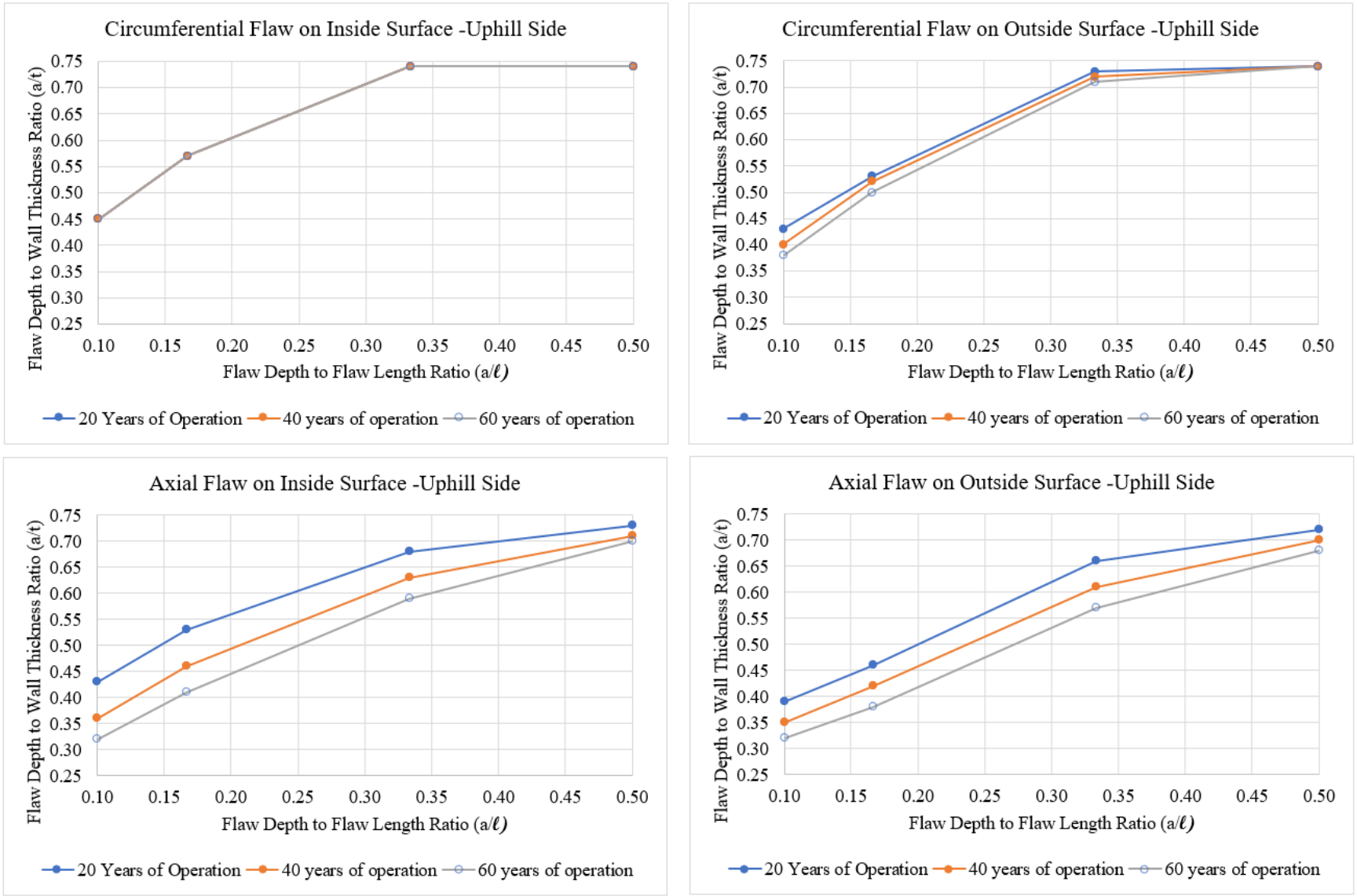

Figure 2-4 Maximum Allowable Initial Flaw Size on CRDM Nozzle for Repair – Uphill Side

3 TECHNICAL BASIS FOR APPLICATION OF EMBEDDED FLAW REPAIR TECHNIQUE TO ATTACHMENT J-GROOVE WELD

This section provides a discussion on the technical basis for the use of the embedded flaw repair method for the flawed head attachment weld (Scenario 2). Such a repair method would involve depositing Alloy 52/52M repair weld material over the wetted surface of the attachment J-groove weld in order to seal it from the primary water environment. At least three weld layers of the Alloy 52/52M repair weld material are deposited (360° full circumference) covering the wetted surface of the penetration nozzle J-groove weld including at least 0.5 inches past the J-groove weld buttering and the stainless steel cladding interface. In addition, at least two layers covering the entire outside surface of the head penetration nozzle below the J-groove weld toe are deposited. [

]^{a,c,e} A flaw evaluation was carried out by analyzing a planar flaw in the reactor vessel head the size of the J-groove weld size.

3.1 ACCEPTANCE CRITERIA

3.1.1 Section XI Appendix K

The evaluation procedure and acceptance criteria used to demonstrate structural integrity of the reactor vessel closure head is contained in Appendix K of ASME Section XI Code [2] as well as Regulatory Guide 1.161 [12]. Although the original purpose of Appendix K was to evaluate reactor vessels with low upper shelf fracture toughness, the general approach in paragraph K-4220 is equally applicable to any region of the reactor vessel where the fracture toughness can be described with elastic plastic parameters. This approach to evaluate the integrity of a nuclear vessel has been developed over several years and has been illustrated with a number of example problems [13] to demonstrate its use. The extension of this methodology to issues other than the low shelf fracture toughness issue is appropriate when service conditions (temperature) promote ductile behavior. The closure head region of the reactor vessel has the operating temperature of about 557 ºF. This would result in ductile behavior and therefore the use of elastic-plastic fracture mechanics method is appropriate.

The acceptance criteria are to be satisfied for each category of transients, namely, Service Load Level A (normal), Level B (upset, including test), Level C (emergency) and Level D (faulted) conditions and two criteria discussed below must be satisfied.

The first criterion is that the crack driving force must be shown to be less than the material toughness as follows:

$$J_{applied} < J_{material}$$

where $J_{applied}$ is the J-integral value calculated for the postulated flaw under the applicable Service Level condition and $J_{material}$ is the J-integral characteristic of the material resistance to ductile tearing at a crack extension of 0.1 inch. For Level A and B conditions, a safety factor of 1.15 is conservatively applied to the $J_{applied}$ per Reg Guide 1.161 [12] and ASME Section XI Appendix K Article K-4220 of ASME Section XI Code [2]. The factor of 1.15 needs only to be applied on pressure, however, in this evaluation it is applied

to the J-integral calculated from the transient and residual stresses in addition to the normal operating pressure. For Level C and D conditions, the safety factor on $J_{applied}$ is 1.0.

The second criterion is that the flaw must also be stable under ductile crack growth as follows [12, Section 1.1.2]:

$$\frac{\partial J_{applied}}{\partial a} < \frac{dJ_{material}}{da}$$

$$\text{at } J_{applied} = J_{material}$$

where,

$J_{material}$ = J-integral resistance to ductile tearing for the material.

$\frac{\partial J_{applied}}{\partial a}$ = Partial derivative of the applied J-integral with respect to flaw depth, a

$\frac{dJ_{material}}{da}$ = Slope of the J-R curve

For Level A and B conditions, a safety factor of 1.25 is conservatively applied to the $J_{applied}$ per Reg Guide 1.161 [12] and ASME Section XI Appendix K Article K-4220 of ASME Section XI Code [2]. The factor of 1.25 needs only to be applied on pressure, however, in this evaluation it is conservatively applied to the transient and residual stresses in addition to the normal operating pressure. For Level C and D conditions, the safety factor on $J_{applied}$ is 1.0. Flaw stability is verified when the slope of the applied J-integral curve is less than the material J-integral curve at the point on J-R curve where the two curves intersect.

3.1.2 Primary Stress Limits

In addition to satisfying the Section XI criteria, the primary stress limits of paragraph NB-3000 in Section III of the ASME Code [14] must be satisfied. The effects of a local area reduction that is equivalent to the area of the postulated flaw in the vessel head attachment weld must be considered by increasing the membrane stresses to reflect the reduced cross section. The allowable flaw depth was determined by evaluating the primary stress of the spherical head with reduced wall thickness using the maximum pressure of [ ]^{a,c,e} for all service conditions. The results show the allowable flaw depth is 2.472 inches.

3.2 METHODOLOGY

Since the depth of a flaw in the attachment weld cannot be detected using current technology, the engineering evaluation for the embedded flaw repair process was performed to demonstrate the stability of an assumed hypothetical flaw that encompasses the entire attachment J-groove weld region in the reactor vessel head near the penetration nozzle. The criteria used to demonstrate the stability and structural integrity of the reactor vessel closure head is described in Section 3.1.1 as per the ASME Code [2] and Regulatory Guide 1.161 [12].

After the implementation of the embedded flaw repair process, the only mechanism for sub-critical crack growth is fatigue. Thus, FCG evaluations for the postulated flaws in the reactor vessel head were performed to demonstrate the structural integrity of the repair weld considering the fatigue crack growth of the flaw.

That is, the flaw depth at the end of evaluation period should be below the 2.472 inches as determined in Section 3.1.2 such that primary stress limit of the ASME Code Section III, paragraph NB-3000 [14] is satisfied. In addition, it needs to be shown that the postulated flaw will not grow through the repair layer.

3.2.1 Geometry and Material

The reactor vessel head is made of low alloy carbon steel SA-533 Grade B Class 1 (per [5.f] and FSAR, Table 5-6 [9]) with the following geometry:

[

]^{a,c,e}

The reactor vessel upper head nozzle attachment weld geometry for the nozzles used in this calculation is tabulated in Table 3-1 for the case without the weld fillet as shown in Figure 3-1. The weld dimensions in Table 3-1 are used for the fatigue crack growth and J-integral analyses for postulated flaws in the reactor vessel head. The height and width of the J-groove weld configurations are based on the design dimensions where the weld depths for all penetration nozzles on the uphill and downhill sides are provided based on drawing [5.a]. The weld depth dimension 'a', as shown in Figure 3-1 and Table 3-1 are the weld depths without the fillet weld. For the embedded flaw FCG through the repair layer, a nominal fillet is considered in the analyses that is representative for the Catawba Unit 2 geometry based on review of other similar head geometries. The weld dimensions in Table 3-1 are used in the fatigue crack growth analysis for the growth of postulated flaws through the weld repair layer. [

]^{a,c,e} these flaw depths with the addition of a nominal fillet bound all penetration row weld depths 'a' for Catawba Unit 2.

Table 3-1 J-Groove Weld Geometries-Without Weld Fillet

a,c,e

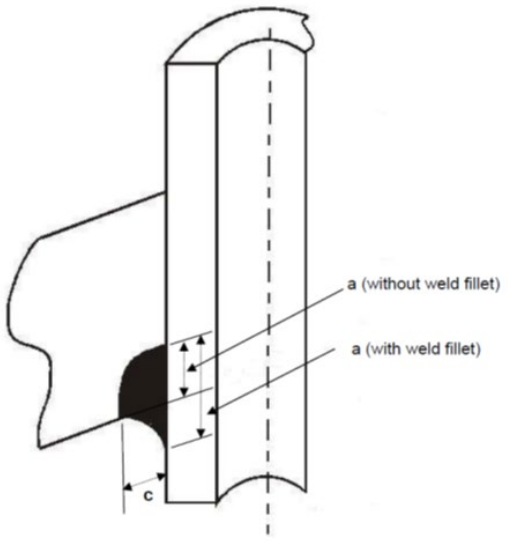

Figure 3-1 Definition of J-Groove Weld Dimensions

3.2.2 Loading Conditions

For the normal/upset condition, the reactor vessel closure head structural integrity evaluation is performed for all the transients in Table 2-1, and [

]^{a,c,e} For the emergency and faulted condition evaluation, [

]^{a,c,e}

There are many head penetrations in the reactor vessel upper head, and [

]^{a,c,e} The distribution of residual, transient thermal, and pressure stresses in the closure head region is obtained from detailed three-dimensional elastic-plastic finite element analyses of the head penetration nozzle region [6]. [

]^{a,c,e}

3.2.3 Stress Intensity Factors

J-Groove Weld Double Corner Crack in the Reactor Vessel Head

Since the depth of a flaw in the attachment weld cannot be detected using current technology, it is conservatively assumed that the flaw in the attachment weld extends radially over the entire attachment weld. [

]^{a,c,e}

The stress intensity factor expression shown above is applicable for a range of flaw shapes, with the depth of the flaw defined as “a”, and the width of the flaw defined as “c”, as shown in Figure 3-2. This flexibility is necessary because this expression can be applied to different attachment J-groove weld shapes for Catawba Unit 2 closure head penetrations as shown in Table 3-1. The attachment J-groove weld shapes were based on the J-groove geometry shown in the head penetration nozzle drawings and models for Catawba Unit 2 [5.a]. [

]^{a,c,e}

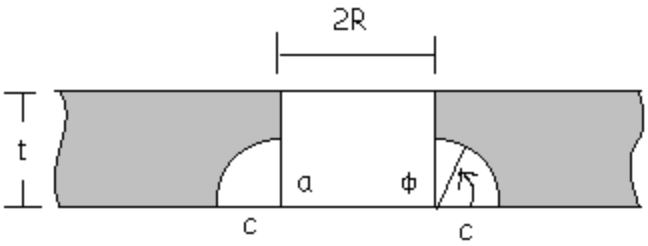

Figure 3-2 Corner Crack Geometry

Embedded Flaw in the Reactor Vessel Head

Fatigue crack growth analyses will also be performed for an embedded flaw after the J-groove weld repair is performed for the nozzles. [

]^{a,c,e} The details of the method is discussed in Section 2.2.5.

3.2.4 J-R curve for Reactor Vessel Closure Head Material

One of the most important pieces of information for fracture toughness for pressure vessel and piping materials is the J-R curve of the material. The "J-R" stands for material resistance to crack extension, as represented by the measured J-integral value versus crack extension. Simply put, the J-R curve to cracking resistance is as significant as the stress-strain curve to the load-carrying capacity and the ductility of a material. Both the J-R curve and stress-strain curves are properties of a material.

[

]^{a,c,e}

Neutron irradiation has been shown to produce embrittlement that reduces the toughness properties of the reactor vessel ferritic steel material. The irradiation levels are very low in the reactor vessel closure head region and therefore the fracture toughness will not be measurably affected.

3.2.5 Applied J-Integral

For small scale yielding, $J_{applied}$ of a crack can be calculated by the Linear Elastic Fracture Mechanics (LEFM) method based on the crack tip stress intensity factor, K_I, calculated as per Section 3.2.3. However, a plastic zone correction must be performed to account for the plastic deformation at the crack tip similar to the approach in Regulatory Guide 1.161 [12]. The plastic deformation ahead of the crack front is then regarded as a failed zone and the crack size is, in effect, increased. The K_I-values can be converted to $J_{applied}$ by the following equation:

$$J_{applied} = \frac{K_{ep}^2}{E'}$$

where K_{ep} is the plastic zone corrected K-value, and $E'=E/(1-\nu^2)$ for plane strain, E = Young's Modulus, and ν = Poisson's Ratio.

K_{ep} is equal to the elastically calculated K_I-value based on the plastic zone adjusted crack depth or size. The plastic zone size, r_p, is calculated by

$$r_p = \frac{1}{6\pi}\left(\frac{K_I}{S_y}\right)^2$$

where S_y is the yield strength of the material.

Assume that the crack depth is a_o, the K_{ep} can now be calculated based on a new crack length, $a_o + r_p$. For small scale yielding, this can be simplified as

$$K_{ep} = f\, K_I$$

where $f = \sqrt{\frac{(a_o+r_p)}{a_o}}$

Once the J-applied is calculated, stability for the postulated flaw in the attachment J-groove weld can be determined using the methodology described in Section 3.1.1.

3.2.6 Fatigue Crack Growth Prediction

With the application of the embedded flaw repair process, any postulated flaws in the reactor vessel head penetration tubes or the attachment weld are sealed from the PWR environment; therefore, the only mechanism for crack growth would be due to fatigue.

The FCG analysis procedure involves postulating an initial flaw at the region of concern and predicting the growth of that flaw due to an imposed series of loading transients, using the same approach described in Section 2.2.6. The FCG curves used for [

]^{a,c,e} and the embedded flaw beneath the repair weld are discussed below.

FCG Curve for the Reactor Vessel Closure Head: Carbon and Low Alloy Ferritic Steel

The crack growth rate curves used in the analyses for [

]^{a,c,e} are taken directly from Appendix A in the ASME Section XI Code [2] for ferritic steel material. With the repair weld any potential flaws in the J-groove weld (Alloy 182) are sealed from the primary water environment and the only applicable growth mechanism is fatigue crack growth in air environment; therefore, the analysis is performed for a surface flaw based on the limiting crack growth rate reference curve of the air environment. This curve is a function of the applied stress intensity factor range (ΔK_I) and the R ratio, which is the ratio of the minimum to maximum stress intensity factor during a thermal transient. The crack growth equation is given below:

$$\frac{da}{dN} = C_0(\Delta K_I)^n$$

where n is the slope of the log (da/dN) versus log (ΔK_I) curve and is equal to 3.07 for subsurface flaws.

Parameter C_o is a scaling constant:

$$\begin{aligned} C_0 &= 0 && for\ \Delta K_I < \Delta K_{th} \\ &= 1.99 \times 10^{-10} S && for\ \Delta K_I \geq \Delta K_{th} \end{aligned}$$

where ΔK_{th} is the threshold ΔK_I value below which the fatigue crack growth rate is negligible and S is a scaling parameter. Both ΔK_{th} and S are a function of the R ratio (K_{min}/K_{max}). The calculation of crack tip stress intensity factor range (ΔK_I) also changes with R ratio when $\Delta K_I \geq \Delta K_{th}$.

$$\begin{aligned} \Delta K_{th} &= 5.0 && for\ R < 0 \\ &= 5.0(1 - 0.8R) && for\ 0 \leq R < 1.0 \end{aligned}$$

The calculation of crack tip stress intensity factor range (ΔK_I) also changes with R ratio when $\Delta K_I \geq \Delta K_{th}$. The calculation of S and ΔK_I for different R ratio ranges is summarized below:

- For $0 \leq R \leq 1$

  $S = 25.72(2.88\text{-}R)^{-3.07}$ and $\Delta K_I = K_{max} - K_{min}$

- For $R < 0$ and $K_{max} - K_{min} > 1.12\sigma_f\sqrt{\pi a}$

  $S=1$ and $\Delta K_I = K_{max} - K_{min}$

- For $-2 \leq R \leq 0$ and $K_{max} - K_{min} \leq 1.12\sigma_f\sqrt{\pi a}$

  $S=1$ and $\Delta K_I = K_{max}$

- For $R<-2$ and $K_{max} - K_{min} \leq 1.12\sigma_f\sqrt{\pi a}$

  $S=1$ and $\Delta K_I = (1\text{-}R)K_{max}/3$

[

]a,c,e

Note that a condition is imposed on A-4300(b)(1) of ASME Code Section XI in 10CFR 50.55a Codes and Standards and a factor of 0.8 is applied to the limit in $K_{max} - K_{min}$ defined in A-4300 of the ASME Code Section XI [2].

FCG Curve for the Repair Weld, Alloy 52/52M, Below the J-Groove Attachment Weld

[

]a,c,e

3.3 FRACTURE MECHANICS ANALYSIS RESULTS

3.3.1 Results for Applied J-Integral and J-R Curve

For the J-integral calculation, the key aspects of the analysis are to demonstrate that the magnitude of J-applied is less than J-material at 0.1 inch crack extension, and the slope of the J-material curve is greater than the slope of the J-applied curve at the intersection of the J_{mat} and $J_{applied}$ curves. This evaluation is performed for the postulated flaws encompassing the J-groove welds at all the nozzle locations. The weld dimensions are shown in Table 3-1. The results shows that for all the nozzle locations, the applied J-integral is less than material J-integral at 0.1 inch crack extension, as shown in Table 3-2 and Table 3-3. The slope of the J-material curve is also greater than the slope of the J-applied curve at the intersection of the J-applied and J-material curves for all the locations. Figures 3-3 and 3-4 show the plots for the penetration nozzle locations with the highest J-applied at 0.1 inch crack extension for Level A/B and Level C/D conditions, respectively.

Table 3-2 J-Integral Results for 0.1 inch Crack Extension on Downhill and Uphill Sides – Level A/B

Pen. No.	Penetration Angle	Downhill		Uphill	
		$J_{applied}$ (kip-in/in^2)	$J_{material}$ (kip-in/in^2)	$J_{applied}$ (kip-in/in^2)	$J_{material}$ (kip-in/in^2)
1	0.0	0.418	1.415	0.723	1.415
2-5	11.4	0.445	1.415	0.675	1.415
6-9	16.2	0.456	1.415	0.651	1.415
10-13	18.2	0.462	1.415	0.641	1.415
14-17	23.3	0.485	1.415	0.612	1.415
18-21	24.8	0.491	1.415	0.612	1.415
22-29	26.2	0.496	1.415	0.604	1.415
30-37	30.2	0.513	1.415	0.580	1.415
38-41	33.9	0.536	1.415	0.567	1.415
42-49	35.1	0.542	1.415	0.560	1.415
50-53	36.3	0.548	1.415	0.554	1.415
54-61	38.6	0.561	1.415	0.542	1.415
62-65	44.3	0.596	1.415	0.516	1.415
66-73	45.4	0.610	1.415	0.511	1.415
74-78	48.7	0.636	1.415	0.493	1.415

Table 3-3 J-Integral Results for 0.1 inch Crack Extension on Downhill and Uphill Sides – Level C/D

Pen. No.	Penetration Angle	Downhill		Uphill	
		$J_{applied}$ (kip-in/in^2)	$J_{material}$ (kip-in/in^2)	$J_{applied}$ (kip-in/in^2)	$J_{material}$ (kip-in/in^2)
1	0.0	0.497	1.471	1.114	1.471
2-5	11.4	0.530	1.471	0.959	1.471
6-9	16.2	0.545	1.471	0.912	1.471
10-13	18.2	0.551	1.471	0.891	1.471
14-17	23.3	0.581	1.471	0.836	1.471
18-21	24.8	0.587	1.471	0.839	1.471
22-29	26.2	0.594	1.471	0.823	1.471
30-37	30.2	0.614	1.471	0.780	1.471
38-41	33.9	0.645	1.471	0.759	1.471
42-49	35.1	0.652	1.471	0.748	1.471
50-53	36.3	0.660	1.471	0.737	1.471
54-61	38.6	0.675	1.471	0.718	1.471
62-65	44.3	0.720	1.471	0.679	1.471
66-73	45.4	0.737	1.471	0.672	1.471
74-78	48.7	0.770	1.471	0.646	1.471

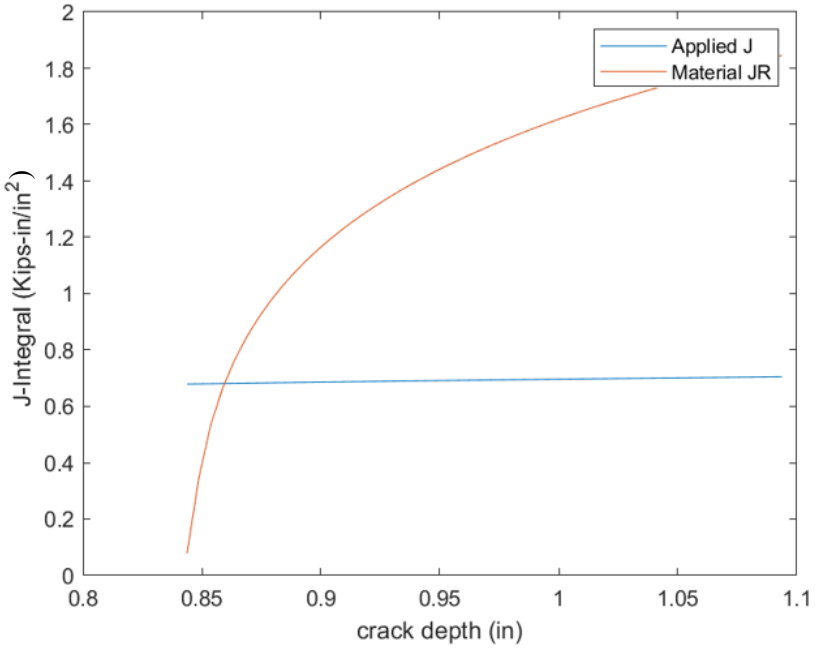

Figure 3-3 Applied and Material J-Integral versus Crack Depth Curve for the Downhill Case with the Highest $J_{applied}$ at 0.1 inch Crack Extension – Level A/B Conditions

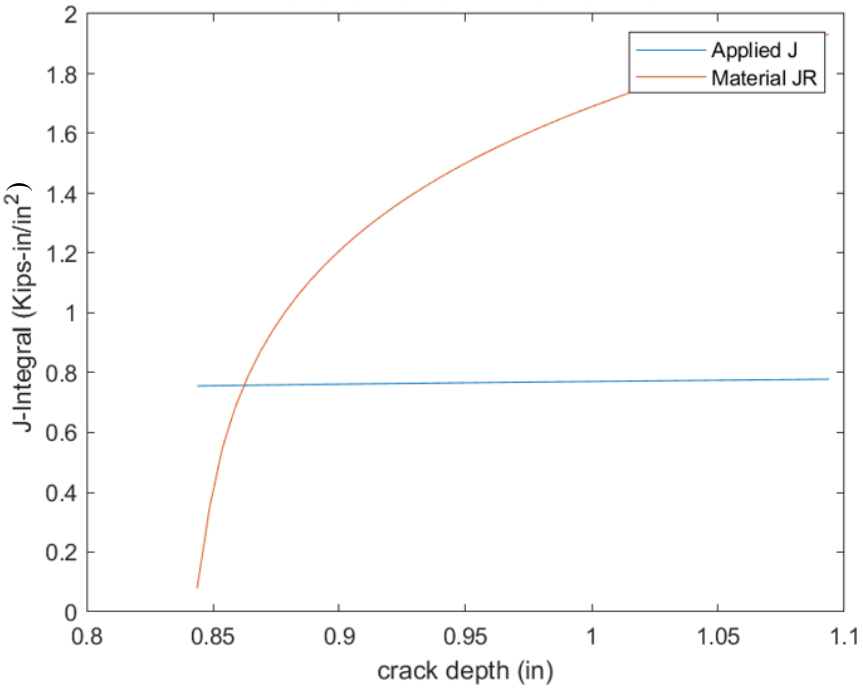

Figure 3-4 Applied and Material J-Integral versus Crack Depth Curve for the Downhill Case with the Highest $J_{applied}$ at 0.1 inch Crack Extension – Level C/D Conditions

3.3.2 Results for Fatigue Crack Growth into the Reactor Vessel Head

The FCG into the reactor vessel head is considered for the postulated cracks with the initial flaw size based on the J-groove weld depth from Table 3-1.

The fatigue crack growth is performed for the outermost nozzle along with the largest J-groove weld dimensions, in order to bound all the other penetration nozzles. It is assumed that the initial aspect ratio is held constant as the flaw grows through the reactor head wall thickness.

The stress intensity factor is conservatively calculated based on [ ]^{a,c,e} and the fatigue crack growth law for the reactor vessel head carbon steel material described in Section 3.2.6 is used. The FCG results are shown in Figure 3-5, which demonstrates that the postulated flaw will not reach the reactor vessel head primary stress limit (2.472 inches) after 60 years of growth.

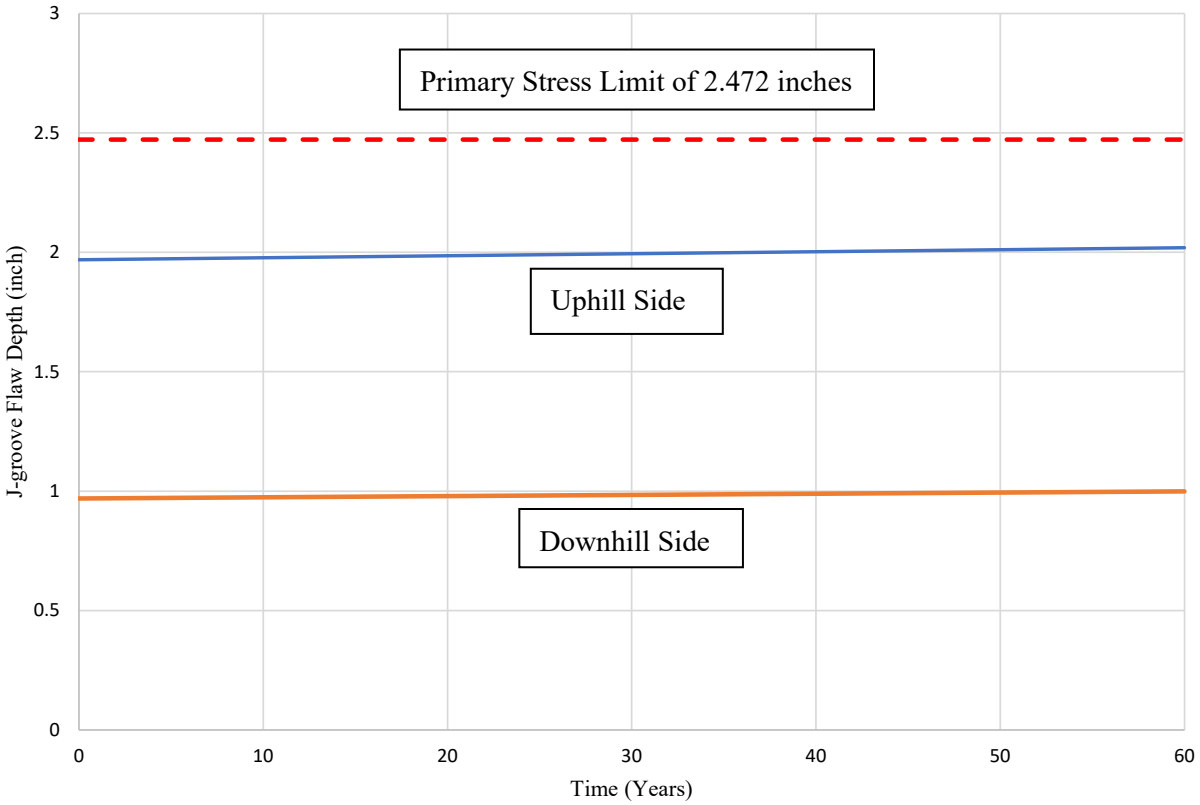

Figure 3-5 Fatigue Crack Growth Prediction into the Reactor Vessel Shell for Postulated Flaws in the J-Groove Welds for the Bounding Penetration Angles on the Downhill and Uphill Sides

3.3.3 Results for Fatigue Crack Growth into the Repair Weld

The attachment weld (J-groove) repair is performed by [

]^{a,c,e} The attachment weld is thus sealed, and the thickness of the reactor vessel shell is locally increased by [ ]^{a,c,e} In order to determine the durability of the repair weld, an embedded flaw based on the J-Groove weld geometry is postulated, which starts from [ ]^{a,c,e} beneath the free surface. The postulated flaw, which encompasses the entire shape of the J-groove weld, will have an aspect ratio (flaw length/flaw depth) of 2. This aspect ratio of 2 bounds all the aspect ratios for the uphill and downhill side attachment weld dimensions shown in Table 3-1. For the FCG analysis, the initial total flaw depth (2a) is assumed equal to the maximum uphill and downhill weld depths [

]^{a,c,e} in Table 3-1. The crack growth results are summarized in Table 3-4 and it shows that the structural integrity of the repaired weld layer is expected to be maintained for at least 47 years of service life.

Table 3-4 Growth of Embedded Flaw in J-Groove Weld

Location	Year	Remaining Repair Weld Thickness (inch)
Uphill Side	0	[ ]^{a,c,e}
	10	[ ]^{a,c,e}
	20	[ ]^{a,c,e}
	30	[ ]^{a,c,e}
	40	[ ]^{a,c,e}
	47	[ ]^{a,c,e}
Downhill Side	0	[ ]^{a,c,e}
	10	[ ]^{a,c,e}
	20	[ ]^{a,c,e}
	30	[ ]^{a,c,e}
	40	[ ]^{a,c,e}
	50	[ ]^{a,c,e}
	60	[ ]^{a,c,e}

4 SUMMARY AND CONCLUSIONS

Engineering evaluations were performed to provide plant specific technical basis for the Westinghouse embedded flaw repair process that is associated with the reactor vessel head penetration nozzle inspection and contingency repair program for Catawba Unit 2.

The technical basis for the use of the embedded flaw repair process if unacceptable flaws are detected in the head penetration nozzles is provided in Section 2. Based on the results in Section 2.3, it is determined that unacceptable axial and circumferential flaws detected on the inside surface or outside surface of a head penetration nozzle can be repaired using the embedded flaw repair process by shielding them from the primary water environment. The maximum allowable initial axial and circumferential flaw sizes that can be repaired using the Westinghouse embedded flaw repair process are shown in Table 2-3 and Figures 2-3 and 2-4 for a plant service life up to 60 years.

The technical basis for the use of the embedded flaw repair process if indications or flaws are found in the head penetration attachment J-groove welds is provided in Section 3. Based on the results shown in Section 3.3, the evaluation documented herein has demonstrated that the embedded flaw repair process is a viable method for repairing flaws found in the attachment J-groove weld. The fracture mechanics evaluation demonstrated that a flaw postulated in the J-groove weld which encompasses the entire attachment J-groove weld shape is stable under the J-integral analysis. Furthermore, the reduced wall thickness considering the 60-year fatigue crack growth of the postulated flaw will meet the reactor vessel head primary stress limit minimum thickness requirement. The fatigue crack growth through the weld overlay repair layer demonstrates that a postulated flaw in the J-groove weld will not grow through the repair layer in less than 47 years. Therefore, it is technically justified to use the embedded flaw repair process as the repair option for the reactor vessel head penetration nozzle attachment J-groove welds since the criteria for application of such a process as stated in Appendix C of WCAP-15987-P Revision 2-P-A [4] is met.

5 REFERENCES

1. Duke Energy, RA-21-0145, "Revision to Proposed Alternative to Use Reactor Vessel Head Penetration Embedded Flaw Repair Method," April 24, 2021 (ML21114A000).
2. ASME Boiler & Pressure Vessel Code, 2007 Edition with 2008 Addenda, Section XI, Rules for Inservice Inspection of Nuclear Power Plant Components.
3. Westinghouse Letter, LTR-SDA-19-017, Revision 0, "Catawba Unit 2 General Reactor Vessel Control Rod Drive Mechanism (CRDM) Penetration J-Groove Weld Repair Dimensional Requirements," March 14, 2019.
4. Westinghouse Report WCAP-15987-P, Revision 2-P-A, "Technical Basis for the Embedded Flaw Process for Repair of Reactor Vessel Head Penetrations," December 2003.
5. [

]a,c,e

6. [

]a,c,e

7. [

]a,c,e

8. [

]a,c,e

9. Duke Energy Company, "Catawba Nuclear Station Updated Final Safety Analysis Report," Revision 20, April 2018.
10. [

]a,c,e

11. [

]a,c,e

12. Regulatory Guide 1.161, “Evaluation of Reactor Pressure Vessels with Charpy Upper-Shelf Energy Less Than 50 ft-lb.”

13. “Development of Criteria for Assessment of Reactor Vessels with Low Upper Shelf Fracture Toughness,” Welding Research Council Bulletin 413, July 1996.

14. ASME Boiler & Pressure Vessel Code, 1971 Edition with Addenda through the Winter of 1972, Section III, Rules for Construction of Nuclear Power Plant Component.

15. [

]a,c,e

16. [

]a,c,e

Attachment 3

Affidavit Attesting to Proprietary Nature of Information in Attachment 1

Commonwealth of Pennsylvania:
County of Butler:

(1) I, Camille Zozula, Manager, Regulatory Compliance and Corporate Licensing, have been specifically delegated and authorized to apply for withholding and execute this Affidavit on behalf of Westinghouse Electric Company LLC (Westinghouse).

(2) I am requesting the proprietary portions of WCAP-18708-P, Revision 1 be withheld from public disclosure under 10 CFR 2.390.

(3) I have personal knowledge of the criteria and procedures utilized by Westinghouse in designating information as a trade secret, privileged, or as confidential commercial or financial information.

(4) Pursuant to 10 CFR 2.390, the following is furnished for consideration by the Commission in determining whether the information sought to be withheld from public disclosure should be withheld.

(i) The information sought to be withheld from public disclosure is owned and has been held in confidence by Westinghouse and is not customarily disclosed to the public.

(ii) The information sought to be withheld is being transmitted to the Commission in confidence and, to Westinghouse's knowledge, is not available in public sources.

(iii) Westinghouse notes that a showing of substantial harm is no longer an applicable criterion for analyzing whether a document should be withheld from public disclosure. Nevertheless, public disclosure of this proprietary information is likely to cause substantial harm to the competitive position of Westinghouse because it would enhance the ability of competitors to provide similar technical evaluation justifications and licensing defense services for commercial power reactors without commensurate expenses. Also, public disclosure of the information would enable others to use the information to meet NRC requirements for licensing documentation without purchasing the right to use the information.

(5) Westinghouse has policies in place to identify proprietary information. Under that system, information is held in confidence if it falls in one or more of several types, the release of which might result in the loss of an existing or potential competitive advantage, as follows:

(a) The information reveals the distinguishing aspects of a process (or component, structure, tool, method, etc.) where prevention of its use by any of Westinghouse's competitors without license from Westinghouse constitutes a competitive economic advantage over other companies.

(b) It consists of supporting data, including test data, relative to a process (or component, structure, tool, method, etc.), the application of which data secures a competitive economic advantage (e.g., by optimization or improved marketability).

(c) Its use by a competitor would reduce his expenditure of resources or improve his competitive position in the design, manufacture, shipment, installation, assurance of quality, or licensing a similar product.

(d) It reveals cost or price information, production capacities, budget levels, or commercial strategies of Westinghouse, its customers or suppliers.

(e) It reveals aspects of past, present, or future Westinghouse or customer funded development plans and programs of potential commercial value to Westinghouse.

(f) It contains patentable ideas, for which patent protection may be desirable.

(6) The attached documents are bracketed and marked to indicate the bases for withholding. The justification for withholding is indicated in both versions by means of lower-case letters (a) through (f) located as a superscript immediately following the brackets enclosing each item of information being identified as proprietary or in the margin opposite such information. These lower-case letters refer to the types of information Westinghouse customarily holds in confidence identified in Sections (5)(a) through (f) of this Affidavit.

I declare that the averments of fact set forth in this Affidavit are true and correct to the best of my knowledge, information, and belief. I declare under penalty of perjury that the foregoing is true and correct.

Executed on: 6/9/2022

Signed electronically by
Camille Zozula